Biochemistry

 Volume 30, Number 16 April 23, 1991

Accelerated Publications

Refinement of the NMR Solution Structure of a Protein To Remove Distortions Arising from Neglect of Internal Motion†

Jasna Fejzo,‡,§ Andrzej M. Krezel,§ William M. Westler,§ Slobodan Macura,‡,∥ and John L. Markley*,§

Biochemistry Department, College of Agricultural and Life Sciences, University of Wisconsin, 420 Henry Mall, Madison, Wisconsin 53706, and Faculty of Physical Chemistry, University of Belgrade, 11000 Beograd, POB 550, Yugoslavia

Received January 29, 1991

ABSTRACT: The effect of internal motion on the quality of a protein structure derived from nuclear magnetic resonance (NMR) cross relaxation has been investigated experimentally. Internal rotation of the tyrosine-31 ring of turkey ovomucoid third domain was found to mediate magnetization transfer; the effect led to underestimation of proton–proton distances in its immediate neighborhood. Experimental methods that distinguish pure cross relaxation from chemical exchange mediated cross relaxation were used to separate true distances from distorted ones. Uncorrected and corrected sets of distances, where the corrections took internal motion into account, each were used as input to a distance geometry program for structural modeling. Each set of distances yielded a family of similar (converged) structures. The two families of structures differed considerably (2 Å) in the region of tyrosine-31. In addition, differences as large as 1 Å were observed at other positions throughout the structure. These results emphasize the importance of analyzing the effects of internal motions in order to obtain more accurate NMR solution structures.

Important information about the presence of internal motions in proteins has come from nuclear magnetic resonance (NMR) spectroscopy (Wagner, 1983). By contrast, nearly all NMR solution structure determinations have employed the simplifying assumption that proteins are internally rigid bodies. Multidimensional NMR spectroscopy (Ernst et al., 1987), which has developed into a powerful method for determining structures of macromolecules in solution (Wüthrich, 1986), is based on two experimental steps: the assignment of proton resonances to specific atoms in the covalent structure of the molecule and the determination of distances from each given proton to other protons within a sphere of about 5 Å, as derived from NOE[1] measurements. Additional constraints may be provided by other information such as three-bond coupling constants and inferred hydrogen bonds. Rotations of methyl groups and aromatic rings generally are treated in terms of rigid models, i.e., by the use of "pseudoatoms" and correspondingly relaxed distance constraints (Wüthrich, 1986); other internal motions are generally ignored.

The rigid body approximation has fundamental deficiencies given the presence of internal motions in proteins (Jardetzky, 1980). Rapid (picosecond scale) motions have smaller effects on distances obtained from NOE measurements (Olejniczak et al., 1984; LeMaster et al., 1988; Konig et al., 1990). Motions on slower time scales, however, can lead to large errors in the interpretation of cross-relaxation data (Lane, 1988; Konig et al., 1990). Theoretical approaches to the problem have been discussed. Internal motions such as methyl group rotations and aromatic ring flips have been simulated in various

† This work was carried out at the National Magnetic Resonance Facility at Madison under support from NIH Grants LM04958 and RR02301. Equipment in the facility was purchased with funds from the University of Wisconsin, the NSF Biological Instrumentation Program (Grant DMB-8415048), the NIH Biomedical Research Technology Program (Grant RR02301), NIH Shared Instrumentation Program (Grant RR02781), and the U.S. Department of Agriculture. A.M.K. is a Wharton Predoctoral Fellow.

‡ Faculty of Physical Chemistry, University of Belgrade.

§ Biochemistry Department, University of Wisconsin—Madison.

∥ Present address: Department of Biochemistry and Molecular Biology, Mayo Foundation, 200 First St. SW, Rochester, MN 55905.

[1] Abbreviations: NOE, nuclear Overhauser effect; NOESY, nuclear Overhauser effect spectroscopy; OMTKY3, unglycosylated turkey ovomucoid third domain (the carboxyl-terminal 56 amino acid residues of the full ovomucoid molecule) obtained by limited proteolysis (Bogard et al., 1980); rmsd, root mean square deviation; pH*, uncorrected pH meter reading of a sample dissolved in ^2H_2O.

0006-2960/91/0430-3807$02.50/0

ways, and the cross-relaxation effects have been calculated (Genest, 1989; Torda et al., 1989, 1990; Konig et al., 1990; Yip & Case, 1990). Such studies are model dependent in that they require information about the presence of slow internal motions and their frequencies. In cases where the experimental data can be accommodated only by postulating the presence of two slowly interconverting conformational states, the penalty function for violation of distance constraints can be adjusted so that it is minimized for large distance violations; this procedure can permit convergence to two alternative structures, where most of the distance constraints satisfy both structures but some satisfy only one and not the other (Kim & Prestegard, 1989).

In macromolecules, magnetization exchange by cross relaxation and chemical exchange are formally equivalent (Noggle & Schirmer, 1971; Neuhaus & Williamson, 1989). NOESY (Macura & Ernst, 1980) and other methods used to study cross relaxation do not normally distinguish between the two mechanisms. Since multiple-step magnetization exchange also occurs, five possibilities need to be considered: (1) single-step cross relaxation, (2) multiple-step cross relaxation (spin diffusion), (3) single-step chemical exchange, (4) multiple-step chemical exchange, and (5) multiple-step hybrid mechanisms that involve both cross relaxation and chemical exchange steps. Spin diffusion can be recognized and dealt with by fitting the NOE buildup (Fejzo et al., 1990a) or by taking a full relaxation matrix approach (Keepers & James, 1984; Marion et al., 1987; Lefèvre, et al., 1987; Olejniczak et al., 1986; Boelens et al., 1988; Borgias & James, 1988). Recently methods have been developed for identifying and separating pure cross-relaxation and pure chemical exchange data (Bax, 1988; Fejzo et al., 1990b, 1991). This paper addresses the effects of hybrid exchange mechanisms that have the potential of transferring cross relaxation over long distances. We present methods for removing chemical exchange effects from magnetization exchange experiments (NOESY). These procedures yielded a set of interproton distances that are free from long-range spin diffusion artifacts, which ordinarily are introduced by chemical exchange processes. We report that structures obtained from the set of refined distances differ significantly from those obtained from uncorrected distances.

Materials and Methods

Turkey ovomucoid third domain was prepared as described previously (Robertson et al., 1988). For studies carried out at 5 °C and above, ^2H_2O was used as the solvent; for studies carried out at lower temperatures (and one comparison at 5 °C), a 30/70 mixture of glycerol-d_8/^2H_2O was used. ^1H NMR spectra were obtained at 470 MHz (on a Nicolet NT-470 spectrometer at the Purdue University Magnetic Resonance Facility) and at 500 MHz (on a Bruker AM-500 spectrometer at the National Magnetic Resonance Facility at Madison). Distance constraints derived from the NMR analysis of OMTKY3 (A. M. Krezel, A. D. Robertson, P. Darba, and J. L. Markley, manuscript in preparation) were corrected by using information from NMR experiments that identify and remove effects of chemical exchange mediated spin diffusion (Fejzo et al., 1990, 1991). Chemical exchange mediated spin diffusion was eliminated (i) by dissolving the protein in a 30/70 mixture of glycerol-d_8/^2H_2O and lowering the temperature or (ii) by the exchange-decoupled NOESY (XD-NOESY) experiment (Fejzo et al., 1991). In the latter approach, an unwanted spin diffusion pathway is eliminated by irradiating one or more resonances of the chemically exchanging species (Massefski & Redfield, 1988). The original

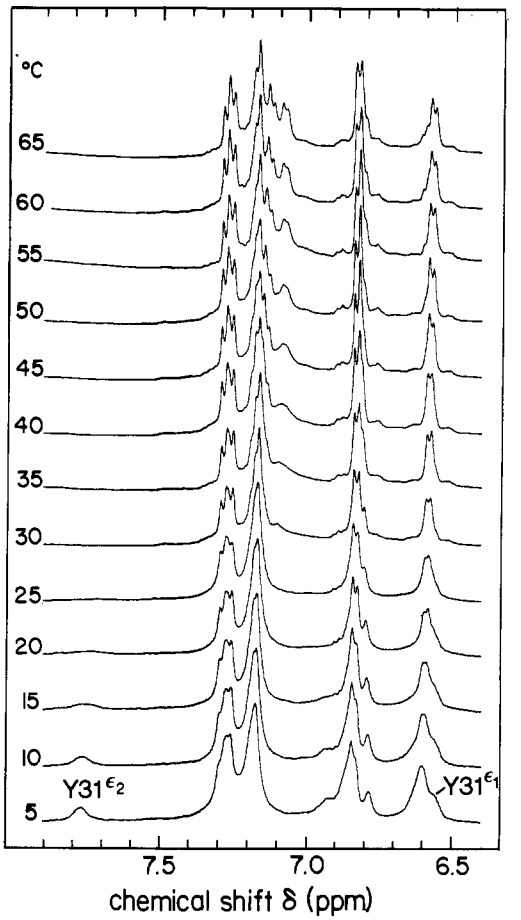

FIGURE 1: One-dimensional ^1H NMR spectra (470 MHz) of OMTKY3 at different temperatures indicated. Resonances from the phenyl ring of Tyr^{31}, which executes 180° ring flips, change their position and shape as a function of the temperature. The protein (5 mM) was dissolved in 0.2 M KCl in ^2H_2O; the pH* was 8.0.

and corrected sets of distance constraints were used as input to a metric-matrix algorithm followed by minimization of distance constraint violations (DSPACE, Hare Research). Twenty convergent structures were calculated with each of the two input data sets. The number of residual violations of distance constraints was similar (<10) among all converged structures, but the two sets of distance constraints yielded two distinct families of structures. The average rmsd for backbone atoms was 0.9 Å for pairwise comparisons of structures generated from the uncorrected distances and 1.1 Å for pairwise comparisons of structures generated from the corrected distances.

Results

Chemical exchange processes that occur at rates comparable to the chemical shift difference between the resonances of the exchanging spins ($\Delta\nu$, expressed in hertz) influence line shapes. This is illustrated (Figure 1) by the aromatic region of the one-dimensional ^1H NMR spectrum of turkey ovomucoid third domain, a small globular protein of M_r 6015. A high-resolution X-ray structure is available for OMTKY3 (Fujinaga et al., 1987), and cross-relaxation pathways in the protein have been investigated extensively (Fejzo et al., 1990a). OMTKY3 serves as a convenient model for the study of protein dynamics because the flip rate of the Tyr^{31} side chain, which serves as a source of internal motion, can be controlled by pH and temperature (Fejzo et al., 1990b). At low temperatures (≤5 °C), where chemical exchange (180° flips of the aromatic ring) is slow on the NMR time scale, each ring proton of Tyr^{31} has

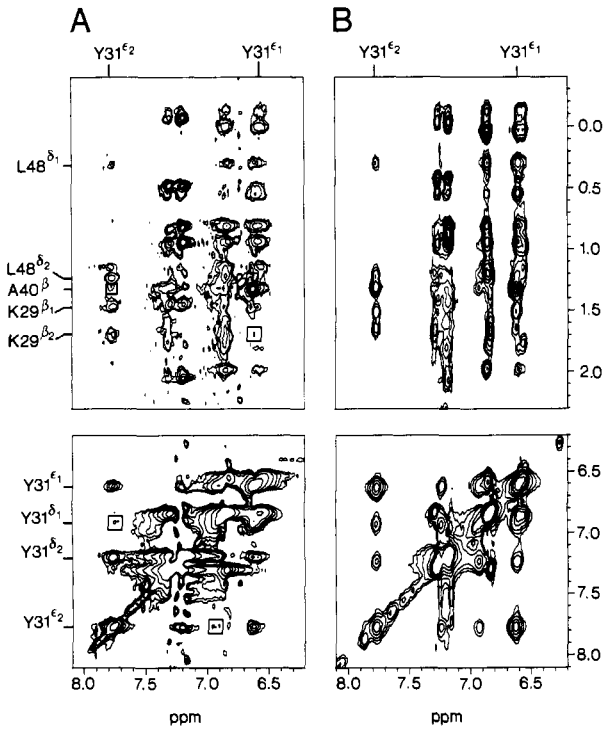

FIGURE 2: Example of the identification of cross peaks that arise from chemical exchange mediated cross relaxation by comparing two-dimensional NOESY spectra (mixing time 20 ms) of OMTKY3 recorded at different temperatures. The protein (5 mM) was dissolved in 30% perdeuterated glycerol/70% ^2H_2O; the pH* was 8.1. (A) At −8 °C, chemical exchange mediated magnetization transfer is comparable to cross relaxation; individual cross peaks arise purely from either cross relaxation or chemical exchange. [Boxes indicate positions at which hybrid (chemical exchange plus cross relaxation) cross peaks appear at higher temperatures.] (B) At +5 °C, chemical exchange is much faster than cross relaxation so that some cross peaks arise from the combination of chemical exchange and cross relaxation. Such cross peaks, if misinterpreted as pure cross-relaxation cross peaks, give false information on the spatial proximity of the nuclei.

its own resonance frequency owing to asymmetry in the chemical environment surrounding the symmetric ring. As the temperature is raised, the protons on the two sides of the ring ($^1H^{\delta1}$ and $^1H^{\delta2}$; $^1H^{\epsilon1}$ and $^1H^{\epsilon2}$) exchange faster between the two chemical environments. At intermediate temperatures (about 25 °C in the present example, Figure 1), the chemical exchange rate and chemical shift difference are comparable, and resonances from the protons undergoing chemical exchange broaden and disappear. Above the coalescence temperature (e.g., 65 °C, Figure 1), the resonances sharpen at the position of the time average of the chemical shifts of the individual exchanging species.

Since resonances from the Tyr^{31} ring protons are not visible at room temperature (ring flips in the coalescence range at 500 MHz), the studies were carried out at low temperatures. By going to subzero temperatures, we were able to decrease the ratio of the rates of chemical exchange and cross relaxation (k/σ) and obtain pure cross-relaxation spectra. At −8 °C (Figure 2A), where the chemical exchange and cross-relaxation rates are comparable, the spectrum contains either pure cross-relaxation lines, whose intensities are a measure of spatial proximity, or chemical exchange lines, whose intensities correlate with rates of internal mobility.

At +5 °C, thermal activation increases the Tyr^{31} ring flip rate, but cross-relaxation rates decrease because the overall rotational correlation time decreases as a result of the lower solution viscosity. Since cross relaxation and chemical exchange are mediated by unrelated processes (overall molecular reorientation and internal molecular flexibility, respectively) their relative magnitudes vary arbitrarily. This means that, for a given k/σ ratio, exchanging resonances may be in a slow, intermediate (coalescence), or fast motion regime as determined by the magnetic field strength, which controls $\Delta\nu$ (in hertz). In a two-spin system, both the chemical exchange and cross-relaxation pathways may be active; the resulting modification of the pure cross-relaxation peak volume is easy to identify and eliminate (Fejzo et al., 1990b, 1991). In a three-spin system (A, B, C), chemical exchange of spins A and B can transmit A magnetization into the cross-relaxation pathway between B and C; this will give rise to a relay cross peak between spins A and C. If the chemical exchange rate is sufficiently fast ($k/\sigma > 10$), this cross peak may be interpreted as a pure cross-relaxation peak, with the incorrect interpretation that spins A and C are in close proximity (short distance r_{AC}). The faster the chemical exchange rate and the larger the distance between the chemically exchanging spins (r_{AB}), the larger the error in the distance r_{AC}.

The degree of interference between chemical exchange and cross relaxation depends solely on the relative magnitudes of k and σ. In the limit when $k/\sigma \gg 10$ and the spins are still in the slow exchange regime ($k/\Delta\nu < 1$) (chemical exchange much faster than cross relaxation), the apparent distance r_{AC} would converge toward r_{BC}, even though $\mathbf{r}_{AC} = \mathbf{r}_{AB} + \mathbf{r}_{BC}$ (vector sum). As an example, the OMTKY3 NOESY spectrum (Figure 2B) contains cross peaks resulting from hybrid magnetization transfer in addition to pure cross-relaxation cross peaks and pure chemical exchange cross peaks. The (Tyr^{31} $^1H^{\epsilon2}$, Ala^{40} $^1H^{\beta}$), (Tyr^{31} $^1H^{\epsilon2}$, Tyr^{31} $^1H^{\delta1}$), and (Tyr^{31} $^1H^{\epsilon1}$, Lys^{29} $^1H^{\beta2}$) cross peaks all are due to successive cross-relaxation and chemical exchange magnetization transfer. The intense (Tyr^{31} $^1H^{\epsilon2}$, Tyr^{31} $^1H^{\delta1}$) cross peak obviously cannot stem from cross relaxation alone, since the distance is too great (4.98 Å), or from chemical exchange alone, since this would require breaking chemical bonds. It arises instead from combined cross relaxation and chemical exchange:

$$Tyr^{31}\ ^1H^{\epsilon2} \xrightarrow{\textit{(cross relaxation)}} Tyr^{31}\ ^1H^{\delta2} \xrightarrow{\textit{(chemical exchange)}} Tyr^{31}\ ^1H^{\delta1}$$

or

$$Tyr^{31}\ ^1H^{\epsilon2} \xrightarrow{\textit{(chemical exchange)}} Tyr^{31}\ ^1H^{\epsilon1} \xrightarrow{\textit{(cross relaxation)}} Tyr^{31}\ ^1H^{\delta1}$$

Alternatively, the presence of chemical exchange can be diagnosed by use of a pulse sequence that provides chemical exchange data without the complication of spin diffusion effects (Fejzo et al., 1990b). Once identified, the effects of chemical exchange on cross relaxation can be eliminated by saturating resonances from the group undergoing chemical exchange (Fejzo et al., 1991). This approach (data not shown) revealed that the (Tyr^{31} $^1H^{\epsilon2}$, Leu^{48} $^1H^{\delta1}$), (Tyr^{31} $^1H^{\epsilon2}$, Leu^{48} $^1H^{\delta2}$), (Tyr^{31} $^1H^{\epsilon1}$, Ala^{40} $^1H^{\beta}$), (Tyr^{31} $^1H^{\epsilon2}$, Lys^{29} $^1H^{\beta1}$), (Tyr^{31} $^1H^{\epsilon2}$, Lys^{29} $^1H^{\beta2}$), and (Tyr^{31} $^1H^{\epsilon1}$, Tyr^{31} $^1H^{\delta1}$) cross peaks arise from spatial proximity but that the (Tyr^{31} $^1H^{\epsilon1}$, Tyr^{31} $^1H^{\epsilon2}$) cross peak arises from flips of the Tyr^{31} ring (Fejzo et al., 1990b).

Errors are introduced in distance estimates when hybrid magnetization transfer cross peaks are misinterpreted as pure cross relaxation. Some of the distances modified by Tyr^{31} ring flips are summarized in Table I. As expected, internal motions cause bogus shortening of distances calculated from NOESY data. For example, at +5 °C the Tyr^{31} $^1H^{\epsilon2}$–Ala^{40} $^1H^{\beta}$ distance estimated from magnetization exchange was 3.8 Å; at −8 °C, where chemical exchange does not mediate magnetization exchange, the same distance was estimated to be larger than 5 Å. Similarly, the uncorrected Tyr^{31} $^1H^{\epsilon1}$–Lys^{29} $^1H^{\beta2}$ distance

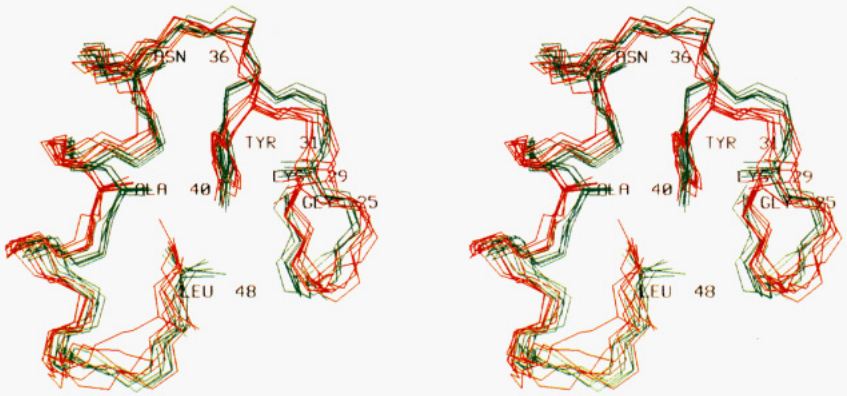

FIGURE 3: Superposition of two families of solution structures of OMTKY3 obtained without (green) and with (red) correction for the internal mobility (ring flips) of the Tyr^{31} ring. For clarity, only the backbone from residues 20 to 48 is shown. Besides changing the local environment of the Tyr^{31} ring, misinterpretation of chemical exchange mediated cross-relaxation peaks as distance constraints led to systematic global changes on the order of 1 Å.

Table I: Comparison of Selected Input and Output Distances from the NMR Solution Structure Determination of Turkey Ovomucoid Third Domain (OMTKY3)[a]

	input distance[b] (Å)		output distance[c] (Å)	
spin pair	uncorr	corr	uncorr	corr
Gly^{25} $^1H^{\alpha 1}$–Tyr^{31} $^1H^{\epsilon 1}$	3.4	>5	3.45	6.24
Lys^{29} $^1H^{\beta 2}$–Tyr^{31} $^1H^{\epsilon 1}$	3.9	>5	4.47	4.73
Tyr^{31} $^1H^{\delta 1}$–Ala^{40} $^1H^{\beta}$	4.8	>6	4.41	6.89
Tyr^{31} $^1H^{\epsilon 1}$–Ala^{40} $^1H^{\beta}$	4.2	4.2	5.04	4.08
Tyr^{31} $^1H^{\epsilon 2}$–Ala^{40} $^1H^{\beta}$	4.8	>6	4.12	6.13
Tyr^{31} $^1H^{\epsilon 1}$–Leu^{48} $^1H^{\delta 2}$	5.7	>6	5.31	7.31

[a] Uncorrected input distance constraints were measured from NOESY spectra. Corrected input distance constraints were obtained from spectra in which chemical exchange effects involving the rotation of the Tyr^{31} rings were suppressed. The output distances represent the respective average interatomic distances in the family of structures calculated with the DSPACE program from either the uncorrected or corrected set of distance constraints. [b] Calculated from NOESY cross-peak intensities. All distances to Ala^{40} $^1H^{\beta}$ include a 1-Å correction to account for rotation of the methyl group (Wüthrich, 1986). [c] From structures derived from distance geometry calculations.

was 3.9 Å; when corrected for internal mobility, it became larger than 5 Å. Since similar corrected distances were determined at +5 °C by the saturation method, the differences arise from differences in the chemical exchange rate rather than a change in the average structure between −8 and +5 °C.

Families of structures derived from the uncorrected and corrected sets of distance constraints are compared in Figure 3. Both local and global differences are evident. Local differences reflect distorted input distances directly, whereas global differences are due to propagation of those distortions by a network of NOEs. Each average distance derived from the set of structures was found to be consistent with the corresponding input distance (Table I) except those for the Tyr^{31} $^1H^{\epsilon 1}$–Ala^{40} $^1H^{\beta}$ and Tyr^{31} $^1H^{\epsilon 2}$–Ala^{40} $^1H^{\beta}$ distances, which deviated in the uncorrected case but not in the corrected case.

In terms of NOE distance constraints, OMTKY3 consists of two subdomains whose local structures are relatively well defined. A smaller number of contraints, many of which involve protons on the side chain of Tyr^{31}, determines the precise relative orientation of the two subdomains. The two sets of distance constraints yielded very similar subdomain structures, except for Tyr^{31} and its immediate surroundings. Interdomain distances, however, were 1 Å shorter, on average, in the structures derived from the set of uncorrected distances than in the structures derived from the set of corrected distances. Many of the global differences found between the two families of structures result from incorrect distances that force the two domains closer to one another when chemical exchange effects are ignored.

Discussion

In two-dimensional exchange spectra (Macura & Ernst, 1980), magnetization transfer (with typical rates of 0.1 to 20 s^{-1}) appears as cross peaks between pairs of proton resonances. If the magnetization exchange arises from pure cross relaxation (dipolar mechanism), cross-peak intensities are functions of the distances between pairs of protons and hence provide information about local geometry. On the other hand, if magnetization exchange is mediated by chemical exchange (internal rotations, ring puckering, etc.) in addition to cross relaxation, the cross peaks have a more complicated origin; if they are misinterpreted as pure cross relaxation, the resulting distances will be in error. NMR solution structures are based mainly on distances estimated from NOESY data (Wüthrich, 1986). The algorithm used to derive the structure, for example, the distance geometry method (Crippen & Havel, 1988), generates one or more structures consistent with the input distance constraints. The resulting structures, whose accuracy reflects the quality of input distances, are often verified by back-calculation of the input NOESY spectrum. However, if some of the input distances were derived from cross peaks with chemical exchange contributions, back-calculation will faithfully reproduce the NOESY spectrum even though the structure is distorted.

The results presented here demonstrate that unrecognized internal mobility can decrease the accuracy of a solution structure determination. The distance errors (Table I) are consistent with those estimated theoretically by considering aromatic ring flips in the framework of the relaxation matrix approach for the calculation of NOE intensities (Konig et al., 1990). The results show that a structure that does not take chemical exchange effects into account can be entirely consistent with observed NOESY spectra, and thus appear to be highly refined, while being inaccurate. Unrecognized chemical exchange can result in local distortions in the vicinity of the mobile group. When exchanging resonances mediate

magnetization transfer between two well-defined structural subdomains, global distortions also will occur.

References

Bax, A. (1988) *J. Magn. Reson. 77*, 134–147.

Boelens, R., Koning, T. M. G., & Kaptein, R. (1988) *J. Mol. Struct. 173*, 299–311.

Bogard, W. C., Jr., Kato, I., & Laskowski, M., Jr. (1980) *J. Biol. Chem. 255*, 6569–6574.

Borgias, B. A., & James, T. L. (1988) *J. Magn. Reson. 79*, 493–512.

Crippen, G. M., & Havel, T. F. (1988) *Distance Geometry and Molecular Conformation*, J. Wiley, New York.

Ernst, R. R., Bodenhausen, G., & Wokaun, A. (1987) *Principles of NMR in One and Two Dimensions*, Clarendon Press, Oxford, England.

Fejzo, J., Zolnai, Zs., Macura, S., & Markley, J. L. (1990a) *J. Magn. Reson. 88*, 93–110.

Fejzo, J., Westler, W. M., Macura, S., & Markley, J. L. (1990b) *J. Am. Chem. Soc. 112*, 2574–2577.

Fejzo, J., Westler, W. M., Macura, S., & Markley, J. L. (1991) *J. Magn. Reson.* (in press).

Fujinaga, M., Sielecki, A. R., Read, R. J., Ardelt, W., Laskowski, M., Jr., & James, M. N. G. (1987) *J. Mol. Biol. 195*, 397–418.

Genest, D. (1989) *Biopolymers 28*, 1903–1911.

Jardetzky, O. (1980) *Biochim. Biophys. Acta 621*, 227–232.

Keepers, J. W., & James, T. L. (1984) *J. Magn. Reson. 57*, 404–426.

Kim, Y., & Prestegard, J. H. (1989) *Biochemistry 28*, 8792–8797.

Konig, T. M. G., Boelens, R., & Kaptein, R. (1990) *J. Magn. Reson. 90*, 111–123.

Lane, A. N. (1988) *J. Magn. Reson. 78*, 425–439.

Lefèvre, J.-F., Lane, A. N., & Jardetzky, O. (1987) *Biochemistry 26*, 5076–5090.

LeMaster, D. M., Kay, L. E., Brünger, A. T., & Prestegard, J. H. (1988) *FEBS Lett. 236*, 71–76.

Macura, S., & Ernst, R. R. (1980) *Mol. Phys. 41*, 95–117.

Marion, D., Genest, M., & Ptak, M. (1987) *Biophys. Chem. 28*, 235–244.

Massefski, W., Jr., & Redfield, A. G. (1988) *J. Magn. Reson. 78*, 150–155.

Neuhaus, D., & Williamson, M. (1989) *The Nuclear Overhauser Effect in Structural and Conformational Analysis*, VCH Publishers, New York.

Noggle, J. S., & Schirmer, R. E. (1971) *The Nuclear Overhauser Effect. Chemical Applications*, Academic Press, New York.

Olejniczak, E. T., Dobson, C. M., Karplus, M., & Levy, R. M. (1984) *J. Am. Chem. Soc. 106*, 1923–1930.

Olejniczak, E. T., Gampe, R. T., Jr., & Fesik, S. W. (1986) *J. Magn. Reson. 67*, 28–41.

Robertson, A. D., Westler, W. M., & Markley, J. L. (1988) *Biochemistry 27*, 2519–2529.

Torda, A. E., Scheek, R. M., & van Gunsteren, W. F. (1989) *Chem. Phys. Lett. 157*, 289–294.

Torda, A. E., Scheek, R. M., & van Gunsteren, W. F. (1990) *J. Mol. Biol. 214*, 223–235.

Wagner, G. (1983) *Q. Rev. Biophys. 16*, 1–57.

Wüthrich, K. (1986) *NMR of Proteins and Nucleic Acids*, J. Wiley, New York.

Yip, P. G., & Case, D. A. (1990) *Computational Aspects of the Study of Biological Macromolecules by NMR*, Proceedings of the NATO Advanced Research Workshop, I1, Ciocco, Italy, June 3–8, 1990.